Syntheses of Ag/Cu alloy and Ag/Cu alloy core Cu shell nanoparticles using a polyol method

Tsuji, Masaharu
Department of Applied Science for Electronics and Materials, Graduate School of Engineering Sciences, Kyushu University

Hikino, Sachie
Institute for Materials Chemistry and Engineering, Kyushu University

Tanabe, Ryuichi
Department of Energy Science and Engineering, Faculty of Engineering, Kyushu University

Matsunaga, Mika
Institute for Materials Chemistry and Engineering, Kyushu University

他

出版情報：CrystEngComm. 12 (11), pp.3900-3908, 2010-11. Royal Society of Chemistry
バージョン：
権利関係：(C) Royal Society of Chemistry 2010

Syntheses of Ag/Cu alloy and Ag/Cu alloy core Cu shell nanoparticles using a polyol method

Masaharu Tsuji,*[a,b,c] Sachie Hikino,[a] Ryuichi Tanabe,[c] Mika Matsunaga[a] and Yoshiyuki Sano[d]

Ag-Cu bimetallic nanoparticles were prepared by reducing mixtures of $AgNO_3$ and $Cu(OAc)_2{\cdot}H_2O$ in ethylene glycol (EG) in the presence of poly(vinylpyrrolidone) (PVP) at 175 ^oC for 5–60 min. At high [Ag]/[Cu] molar ratios of 1 and 2 or at a short reaction time below 5 min, Ag rich Ag/Cu alloy particles were formed. On the other hand, at low [Ag]/[Cu] molar ratios of 0.25 and 0.5 or a long reaction time above ≈15 min, Cu shells were overgrown on Au/Cu cores and new Ag/Cu alloy core Cu shell nanoparticles, denoted as Ag/Cu@Cu, were produced. The formation of Ag/Cu and Ag/Cu@Cu particles was examined using energy dispersed X-ray spectroscopic (EDS) measurements. The growth mechanisms of Ag/Cu and Ag/Cu@Cu particles are discussed on the basis of TEM-EDS and ultraviolet (UV)-visible (Vis)-near infrared (NIR) extinction spectral data. The time dependence of UV-Vis spectra indicated that the Cu component of Ag/Cu@Cu particles has higher antioxidized property for than that of Cu and Cu@Ag particles.

Introduction

Bimetallic nanoparticles have excellent optical, electronic and catalytic properties different from those of the component metals. Therefore much attention has been received for the development of novel synthesis methods of bimetallic nanoparticles and their applications as catalysts, sensors and substrates for surface-enhanced Raman scattering.[1-10] Among many bimetallic nanoparticles, the Ag-Cu bimetallic system has recently received strong attention due to their high electron conductivity and application to lead free past. Although the syntheses of Ag-Cu alloy and core@shell particles have been extensively studied using gas-phase and liquid-phase methods,[11-18] more studied are required to develop simple shape-controlled synthesis methods of Ag-Cu bimetallic particles. In most of previous experiments, crystal structures were characterized using transmission electron microscopic (TEM) and UV-Vis extinction spectral data. However, it was difficult to obtain definite information on crystal structures of Cu-Ag bimetallic particles from dark and bright contrast of TEM images and UV-Vis spectral data. Therefore, TEM-EDS measurements are necessary to determine crystal structures of Ag-Cu bimetallic particles from distributions of Ag and Cu components in each product.

We have recently initiated shape controlled syntheses of Ag-Cu bimetallic nanoparticles. Their crystal structures were determined not only from TEM, high resolution (HR)-TEM and UV-Vis-NIR extinction spectral data but also TEM-EDS data. In our previous studies, we prepared Ag@Cu and Cu@Ag core-shell particles and phase separated Ag/Cu bicompartmental particles by a polyol method.[16-18] When Ag or Cu particles were prepared as seeds and then Cu^{2+} or Ag^+ were added, Ag/Cu bicompartmental particles or Cu@Ag core-shell particles were synthesized, respectively.[16,17] By the addition of $AgNO_3$ to a hot solution of $Cu(OAc)_2{\cdot}H_2O$/EG kept at 175 ^oC, Ag@Cu particles were prepared in high yield (≈100%).[18] Our previous studies demonstrate that whether Ag or Cu seeds are used or what timing two reagents of Ag^+ and Cu^{2+} are added to a solvent strongly affect the crystal structures of final products.

In the present study, we added mixtures of Ag^+ and Cu^{2+} solutions to a hot EG solution in the presence of PVP. Then, we succeeded in the preparation of Ag/Cu alloy and novel Ag/Cu@Cu particles. We found that Ag/Cu alloy or Ag/Cu@Cu particles can be prepared by changing the [Ag]/[Cu] molar ratio or the reaction time. To the best of our knowledge this is the first report on the synthesis of Ag/Cu@Cu particles. The growth mechanisms of Ag/Cu and Ag/Cu@Cu particles prepared in this study and Ag@Cu and Cu@Ag particles synthesized in the previous studies[16,17] are discussed on the basis of TEM–EDS data and selected area electron diffraction (SAED) patterns. The stability of Ag/Cu@Cu particles is examined by monitoring dependence of UV-Vis extinction spectra on the time. It was found that the Cu component of Ag/Cu@Cu particles have higher antioxidization character than that of Cu and Cu@Ag particles.

Experimental

Materials and experimental procedures.

10 mL of 15.9 mM $Cu(OAc)_2{\cdot}H_2O$ in EG, 5 ml of 7.85–62.8 mM $AgNO_3$ in EG, and 10 mL of 477 mM PVP (MW:55,000 in terms of monomer units) in EG were mixed in a 100 mL three-necked flask and Ar was bubbled at room temperature for >20 min to remove oxygen dissolved in the solution. The final concentrations of $Cu(OAc)_2{\cdot}H_2O$, $AgNO_3$ and PVP in EG were 6.36, 1.57–12.56 and 191 mM, respectively. The reagent solutions were soaked in an oil bath preheated at 180 ^oC under bubbling Ar. The temperature profile of solution is shown in Fig. S1 (supplementary information). The solution temperature increases rapidly from a room temperature to about 170 ^oC after heating for about 5 min, slowly increased from 170 to 175 ^oC in the 5–10 min, and it was kept at 175 ^oC above that. The reagent solution was sampled at various reaction times to examine the growth mechanism of product particles. The sample solution was rapidly

cooled in a water bath after a desired reaction time finished.

Characterization of nanoparticles.

Product solutions were centrifuged at 13,000 rpm three times for 15 min each time. The precipitates were collected and then re-dispersed in deionized water. For TEM (JEM-2100XS and JEM-2100F; JEOL) and TEM-EDS observations at an accelerating voltage of 200 kV, samples were prepared by dropping colloidal solutions of the products onto Au grids. Extinction spectra of the product solutions were measured using a spectrometer (UV-3600; Shimadzu Corp.) in the UV-Vis-NIR region.

Results and discussion

Preparation of Ag/Cu bimetallic nanoparticles under various $AgNO_3/Cu(OAc)_2{\cdot}H_2O$ molar ratios.

Fig. 1a-1d depict typical TEM images and their EDS data of product particles obtained at the [Ag]/[Cu] molar ratios of 2, 1, 0.5 and 0.25, respectively. Although it is difficult to distinguish between Ag and Cu components from the dark and bright contrast of TEM images depicted in Fig. 1a-1, 1b-1, 1c-1 and 1d-1, their EDS data show that Ag-Cu bimetallic particles are prepared in high yield. At high [Ag]/[Cu] molar ratios of 2 and 1, the positions of Ag and Cu components coincide well with each other in most particles (Fig. 1a-2~1a-4 and 1b-2~1b-4), although red Cu component is found as partial shells in a few particles. Fig. 2a and 2b portray distributions of the Cu and Ag components along the cross section lines of typical particles shown in Fig. 1a-2 and 1b-2, respectively. These line analysis data show that the ratios of Ag and Cu distributions are nearly constant within one particle. On the other hand, if Ag@Cu core-shell particles are formed using the experimental procedure reported previously,[18] vacancy is observed in the center part of Ag component and the Cu distribution in the two corners are large, as shown in Fig. S2 (supplementary information). The uniform Ag/Cu ratios of the Ag and Cu distributions in the line analysis for more than 15 particles indicated that Ag/Cu alloy particles are dominant products (>95%). The Ag:Cu atomic ratios at the [Ag]/[Cu] molar ratios of 2 and 1 were 78:22 and 76:24%, respectively. These results indicate that Ag rich Ag/Cu alloy particles with similar atomic ratios are prepared under these conditions, independent of

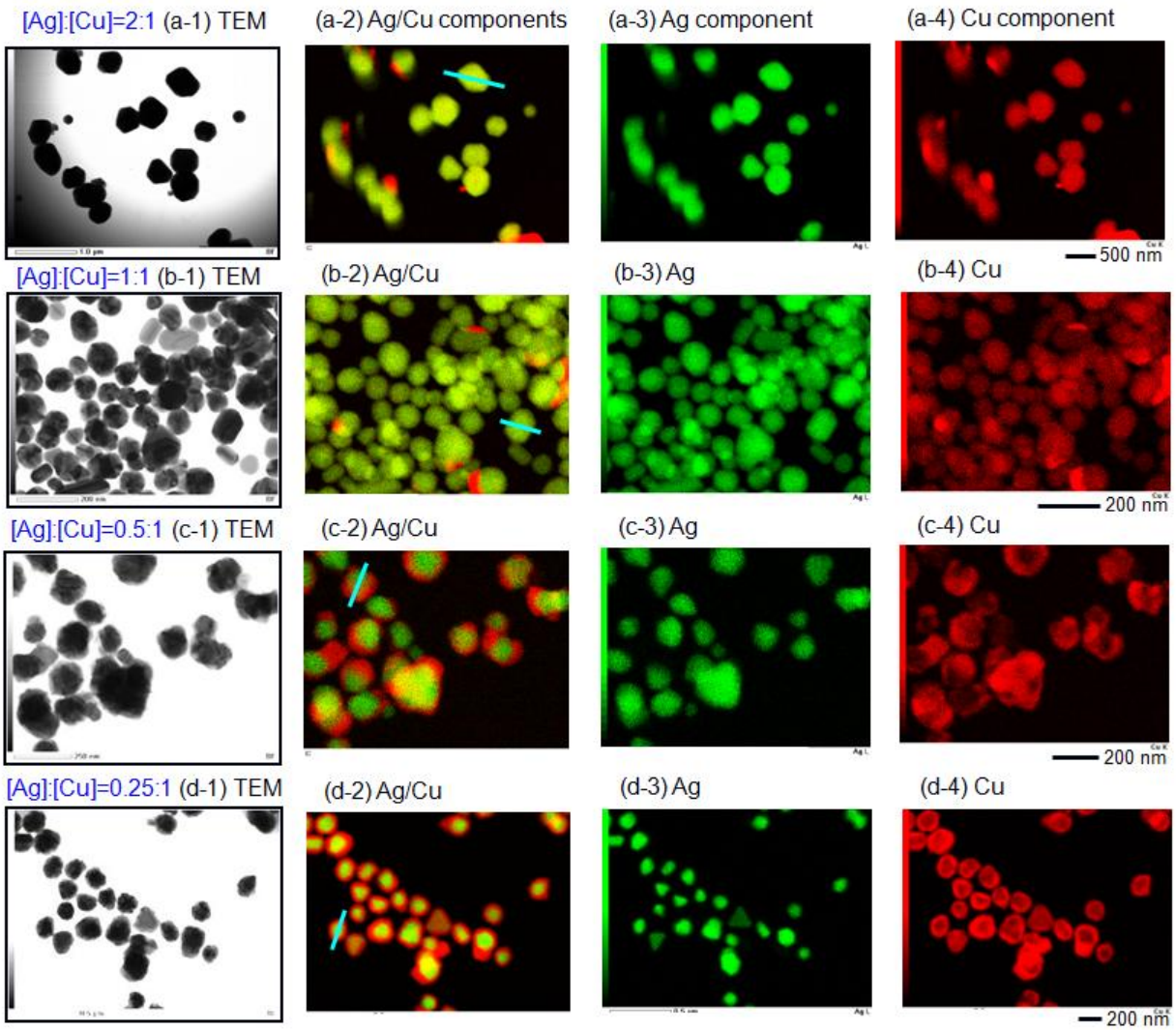

Fig. 1 TEM and TEM-EDS data of Ag-Cu bimetallic particles prepared from $AgNO_3/Cu(OAc)_2{\cdot}H_2O$/PVP mixtures in EG at [Ag]:[Cu] molar ratios of (a) 2:1, (b) 1:1, (c) 0.5:1 and (d) 0.25:1.

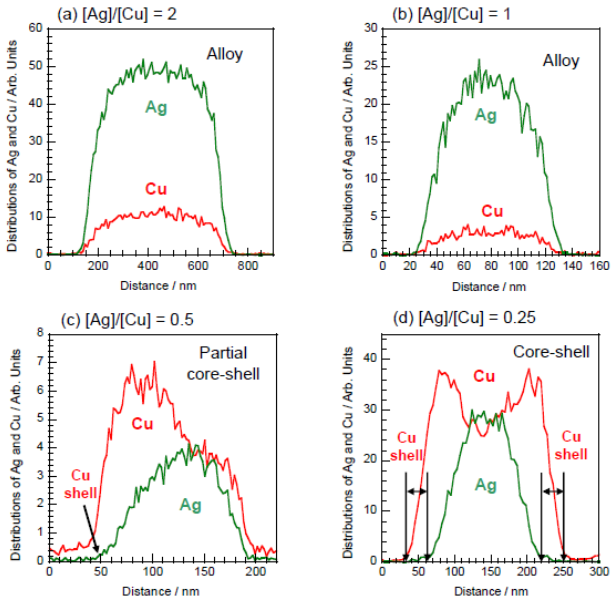

Fig. 2 Distributions of Ag and Cu along cross section lines shown in Fig. 1(a)-1(d).

the [Ag]/[Cu] molar ratio between 2 and 1. The average sizes of Ag/Cu alloy particles were 406±80 and 81±20 nm at the [Ag]/[Cu] molar ratios of 2 and 1, respectively, indicating that the particle size of alloy decreases significantly with decreasing the [Ag]/[Cu] molar ratio.

When the [Ag]/[Cu] molar ratio was reduced to 0.5 and 0.25, different shapes of particles are produced as shown in Fig. 1c and 1d. The average sizes of product particles were 144±85 and 173±48 nm at the [Ag]/[Cu] molar ratios of 0.5 and 0.25, respectively. Although some TEM images shown in Fig. 1c-1 and 1d-1 show dark and bright contrast due to Ag cores and Cu shells, respectively, no definite conclusion can be obtained for the Ag and Cu distributions from the contrast of TEM images for all product particles. On the other hand, EDS data clearly indicate that core-shell particles are produced in high yield (≈100%). Fig. 2c and 2d show the line analysis data of Ag and Cu components along the cross section lines for typical Ag/Cu@Cu particles shown in Fig. 1c-2 and 1d-2, respectively. The distribution of Cu component is not uniform and large in one side in Fig. 2c, whereas a uniform distribution is found in both sides in Fig. 2d. On the basis of the EDS and their line analysis data, it was found that 36±32 nm Cu shells are partially overgrown on Ag rich Ag/Cu alloy core particles as a few Cu shell blocks at an [Ag]/[Cu] molar ratio of 0.5, whereas 40±21 nm Cu shells are fully overgrown on the same core particles at an [Ag]/[Cu] molar ratio of 0.25. The atomic ratios of Ag:Cu components obtained from Ag-Cu particles at the [Ag]/[Cu] molar ratios of 0.5 and 0.25 were determined to be 38:62 and 23:77%, respectively. On the basis of our present data, the Ag/Cu molar ratio decreased with decreasing the [Ag]/[Cu] molar ratio from 1 to 0.25.

Preparation of Ag-Cu bimetallic nanoparticles under various heating times

To obtain more information on crystal growth of Ag/Cu@Cu particles, Ag-Cu bimetallic particles obtained at an [Ag]/[Cu] molar ratio of 0.25 are monitored at various reaction times. Fig. 3a-3c show TEM images and their EDS data obtained at reaction times of 5, 17.5 and 27 min, respectively. The line analysis data of typical particles shown in Fig. 3a-2, 3b-2 and 3c-2 are given in Fig. 4a-4c, respectively. The [Ag]:[Cu] atomic ratios in Fig. 3a-2, 3b-2 and 3c-2 were 88:12, 30:70 and 23:77%, respectively, indicating that the Cu component in the products increases with increasing the reaction time. The EDS data at 5 min suggest that uniform distributions of Ag and Cu components are prepared. These profiles are very similar to those of Fig. 2a and 2b. It is therefore concluded that Ag rich Ag/Cu alloy particles are prepared at 5 min. At 17.5 min, core-shell particles in which Ag/Cu core particles are covered by 23±6.4 nm Cu shells are grown. At 27 min, Ag/Cu core particles are covered by 47±18 nm Cu shells. On the basis of these data, core particles do not consist of pure Ag components but they are composed of Ag rich Ag/Cu components, as obtained at high [Ag]/[Cu] molar ratios of 2 and 1.

The SAED patterns of typical Ag/Cu and Ag/Cu@Cu particles obtained at 5, 17.5 and 27 min were measured (Fig. 5a-5c). At 5 min, many ED spots of (111), (200) and (220) facets of Ag are observed and little spots of Cu are found. At 17.5 min besides above ED spots of Ag, those of (111), (200) and (220) facets of Cu are observed. At 27 min, ED spots of Ag become weak and those of Cu become dominant. These observations are consistent with TEM-EDS data, where Ag rich Ag/Cu alloy particles are initially produced and thick Cu shells are formed with increasing the reaction time. SAED data led us to conclude that Ag/Cu@Cu particles are not amorphous but polycrystals having an fcc type of crystal structure.

Optical properties of Ag/Cu alloy and Ag/Cu@Cu particles.

As an example, Fig. 6a shows color changes of product solution at an [Ag]/[Cu] molar ratio of 0.25. After Ar gas bubbling for 20 min, transparent light blue solution due to $Cu(OAc)_2 \cdot H_2O$ changed to yellowish green. This color change indicates that small Ag particles are produced during Ar bubbling at room temperature. Just after injection of an $AgNO_3/Cu(OAc)_2 \cdot H_2O$/PVP mixture to a hot EG solution (time zero), the solution color starts to change more rapidly. The color became blown, copper, black and copper after heating for 7, 10, 15 and 20 min, respectively. Theses color changes suggest that the contribution of copper increased with increasing the reaction time. Such color changes become slow with increasing the [Ag]/[Cu] molar ratio owing to the decrease in the contribution of the Cu component, as shown in Fig. 6b for the [Ag]/[Cu] molar ratio of 2.

UV-Vis-NIR spectra were measured to characterize optical properties and to examine time evolution of Ag/Cu@Cu particles at [Ag]/[Cu] molar ratios of 2, 1, 0.5 and 0.25 (Fig. 6c-6f). For comparison UV-Vis-NIR spectra of $Cu(OAc)_2 \cdot H_2O$ and typical spherical Ag and Cu particles in EG are also shown in Fig. S3 (supplementary information). Only weak absorption exists >400 nm for $Cu(OAc)_2 \cdot H_2O$, whereas spherical Ag and Cu particles give surface plasmon resonance (SPR) bands with peaks at ≈400 and ≈600 nm, respectively. At an [Ag]/[Cu] molar ratio of 2 (Fig. 6c), a broad band with a peak at ≈460 nm is observed at 5 min. The intensity increases in the 5–25 min range, whereas it decreases in the 25–60 min range. Although the intensity of the SPR band changes with the reaction time, little changes in

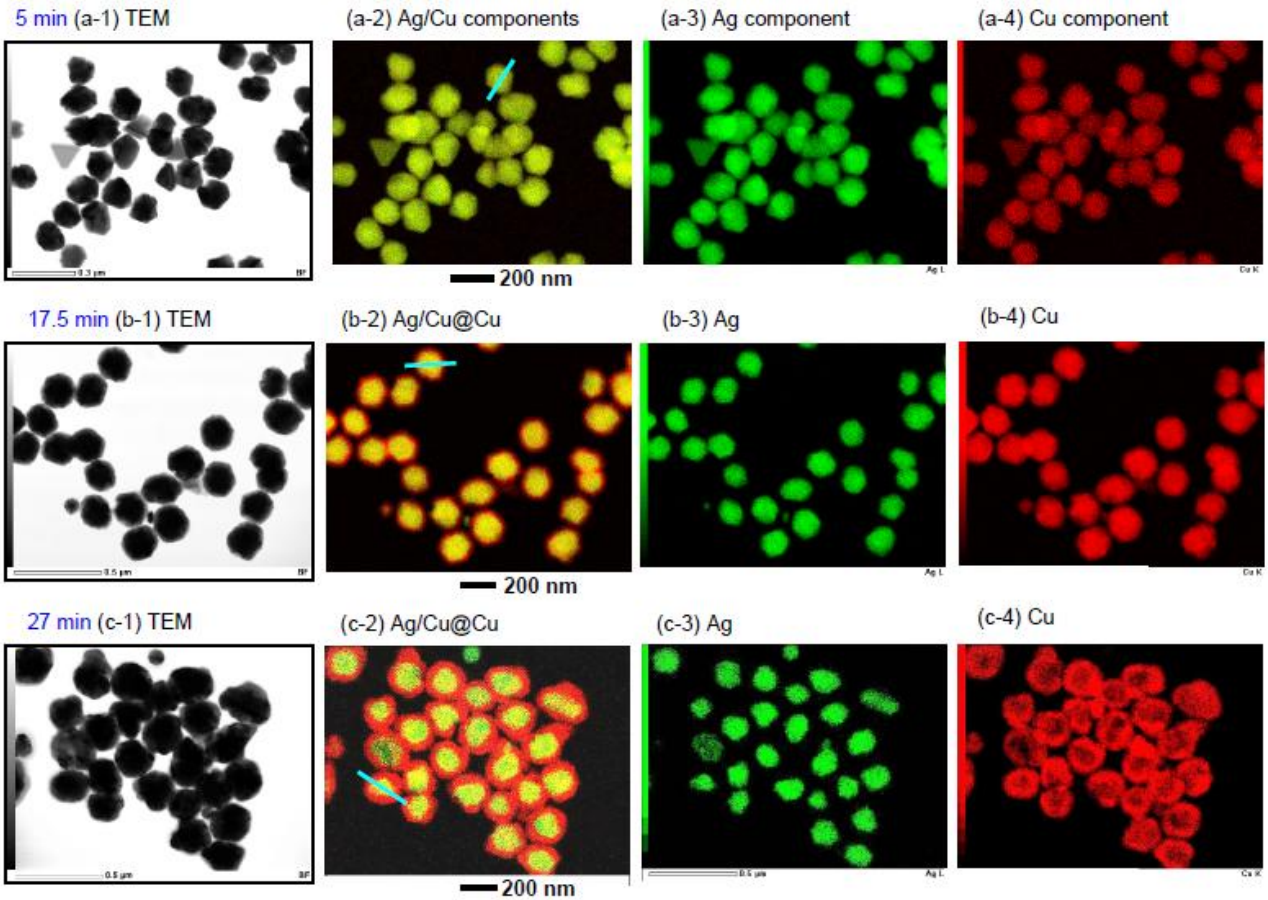

Fig. 3 Ag-Cu bimetallic particles prepared from $AgNO_3$/$Cu(OAc)_2 \cdot H_2O$/PVP mixtures in EG at an [Ag]/[Cu] molar ratio of 0.25 after heating for (a) 5 min, (b) 17.5 min and (c) 27 min.

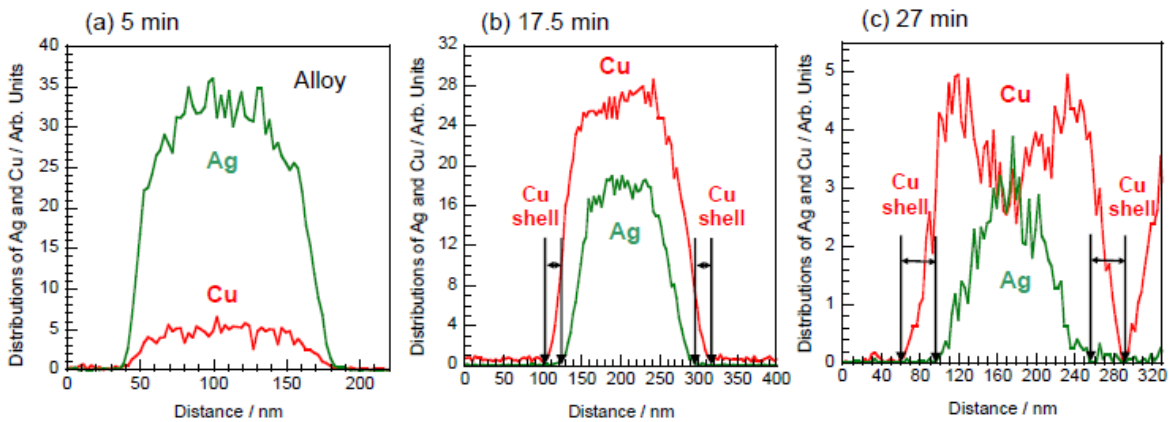

Fig. 4 Distributions of Ag and Cu along cross section lines shown in Fig. 3(a)-3(c).

spectral features are observed. The peak position at ≈460 nm indicates that the contribution of Ag component is large in the Ag rich Ag/Cu alloy. The red shift and broadening of the SPR bands in comparison with those of the pure Ag band (Fig. S3) arise from large particle sizes and their wide size distributions. At an [Ag]/[Cu] molar ratio of 1 (Fig. 6d), a very weak SPR band appears at ≈400 nm owing to the formation of small Ag seeds. During Ar gas bubbling small amount of Ag^+ is reduced to Ag^0 by a weak reducing effect of PVP at a room temperature.[19] After heating for 4.5–14 min, SPR bands with a peak at ≈500 nm appear. The band becomes strong and the peak shifts to blue (≈470 nm) in the 17–25 min range. The peak positions are similar to those observed at an [Ag]/[Cu] molar ratio of 2, although the band widths are narrower than those in Fig. 6c. These spectral characters reflect the facts that the products are similar Ag rich Ag/Cu alloy with smaller sizes and narrower size distributions than those in Fig. 6c. Optical properties of Ag rich Ag/Cu alloys

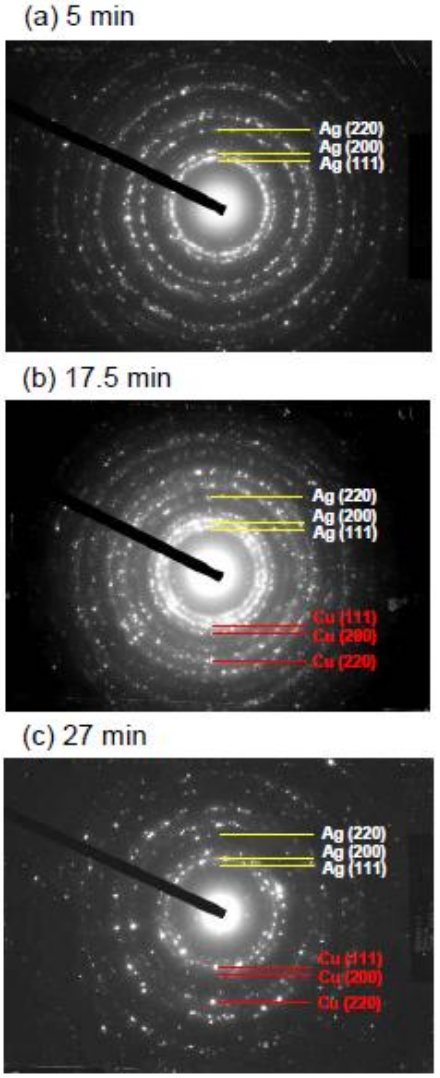

Fig. 5 SEAD patterns of Ag-Cu bimetallic products prepared from $AgNO_3$/$Cu(OAc)_2{\cdot}H_2O$/PVP mixtures in EG at an [Ag]/[Cu] molar ratio of 0.25 after heating for (a) 5 min, (b) 17.5 min and (c) 27 min.

are found to be similar to those of pure Ag particles shown in Fig. S3.

Extinction spectra obtained at [Ag]/[Cu] molar ratios of 0.5 and 0.25 are different from those at 2 and 1 owing to the formation of core-shell structures via Ag/Cu alloy cores. On the basis of detailed data at 0.25 (Fig. 6f), small Ag seeds are initially produced at 0 min during bubbling Ar gas to an $AgNO_3$/$Cu(OAc)_2{\cdot}H_2O$/PVP mixture. After heating for 1.5 min two peaks appear. They become strong and shift to red in the 1.5–17.5 min range. The relative strength of the longer-wavelength component to that of Ag component increases with increasing the reaction time in this time range. At 20–27 min range a strong peak at ≈600 nm corresponding to the Cu component is observed. These spectral changes arise from the formation of Ag rich Ag/Cu alloy core and Cu shell with increasing the reaction time. Similar spectral changes are found at an [Ag]/[Cu] molar ratio of 0.5 (Fig. 6e) owing to the formation of similar Ag/Cu@Cu particles. Outstanding features of the extinction spectra of Au/Cu@Cu particles are that there are two components and the both peaks shift to red with increasing the thickness of Cu shells. This finding indicates that optical property can be controlled by changing thickness of Cu shell by changing the reaction time.

Growth mechanism of Ag/Cu@Cu particles

On the basis of TEM–EDS and UV-Vis-NIR spectral data at various reaction stages, it is reasonable to assume that Ag/Cu@Cu is grown through the following mechanism. Since the standard potential of Cu^{2+}/Cu^0 (+0.34 eV) is relatively low, the reduction rate of Cu^{2+} is slow. On the other hand, since the standard potential of Ag^+/Ag^0 (+0.78 eV) is relatively high, the reduction rate is fast. Therefore, the reduction of Ag^+ occurs more rapidly than that of Cu^{2+} when mixtures of $AgNO_3$ and $Cu(OAc)_2{\cdot}H_2O$ were reduced in EG in the presence of PVP. To reduce Cu^{2+} ions in EG at 175 °C, it takes more than 1 h. However we found that the reduction of Cu^{2+} to Cu^0 was enhanced in the presence of Ag^+. In order to clarify whether Ag^+ or Ag seeded particles are responsible for this effect, we added Ag nanoparticles to $Cu(OAc)_2{\cdot}H_2O$/PVP/EG solution at 175 °C.[20] As a result, the reduction of Cu^{2+} was also enhanced. It was therefore concluded that Ag nanoparticles took part in the enhancement of the reduction of Cu^{2+}. The enhancement of the Cu^{2+} reduction in the presence of Ag particles probably arises from a cathodic polarization of Ag rich Ag/Cu alloy nanoparticles. In the polyol reduction, some organic radicals and electrons are formed as intermediates in the thermal decomposition of EG.[21]

$$CH_2OH\text{-}CH_2OH \rightarrow CH_3CHO + H_2O \quad (1a)$$
$$2CH_3CHO \rightarrow CH_3COCOCH_3 + 2H^+ + 2e^- \quad (1b)$$

The cathodic polarization of Ag/Cu particles by electron transfer from organic radicals and reduction of Cu^{2+} on the surfaces of the Ag rich Ag/Cu alloy particles as found for Sn/Au system[22] may accelerate reduction of Cu^{2+} in the presence of Ag/Cu particles as in the synthesis of Ag@Cu particles.[18] The activation polarization of the $Cu^{2+} + 2e^- \rightarrow Cu^0$ charge-transfer reaction and the diffusion polarization in the mass-transfer process may also participate in the enhancement of reduction of Cu^{2+} on Ag/Cu alloy particles.

We found that atomic Cu % in Ag/Cu alloy was 23±2% at [Ag]/[Cu] molar ratios of 2 and 1. This indicates that Cu solid solubility in Ag is limited at most ≈23% under our conditions. This may be a major reason for a low atomic Cu % in Ag/Cu alloys at the high [Ag]/[Cu] molar ratio range of 1–2. The reduction rate of Ag^+ is much faster than that of Cu^{2+} at 175 °C. Under our conditions, besides the reduction of Ag^+ and Cu^{2+}, (2a) and (2b), the replacement reaction (3) can occur simultaneously.

$$Ag^+ + e^- \rightarrow Ag^0 \quad (2a)$$
$$Cu^{2+} + 2e^- \rightarrow Cu^0 \quad (2b)$$
$$2Ag^+ + Cu^0 \rightarrow Cu^{2+} + 2Ag^0 \quad (3)$$

The reaction (3) oxidized Cu^0 to Cu^{2+} again, so that the reduction rate of Cu^{2+} becomes slow in the presence of Ag^+ and Cu^0. These facts may be other reasons why Ag rich Ag/Cu alloy particles are formed under our conditions.

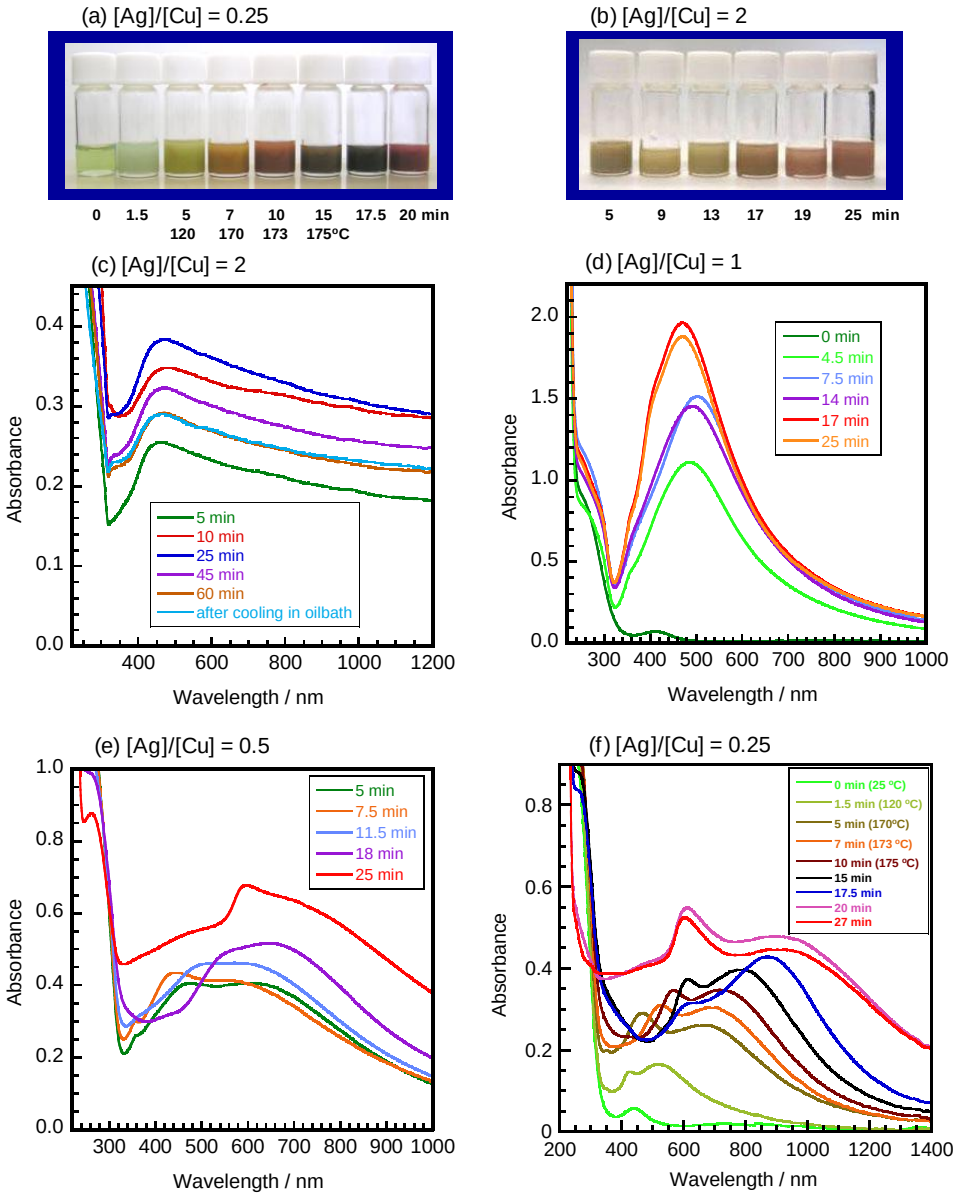

Fig. 6 (a)–(d) Time changes of UV-Vis spectra of Ag/Cu and Ag/Cu@Cu particles obtained at various [Ag]/[Cu] molar ratios after preparation. Similar time changes of (e) Cu and (f) Cu@Ag ([Ag]/[Cu] molar ratio = 0.25) particles are shown for comparison.

At high [Ag]/[Cu] molar ratios of 2 and 1, there are little excess amounts of Cu, so that Ag rich Ag/Cu alloys are produced and little core-shell particles are formed. On the other hand, at low [Ag]/[Cu] molar ratios of 0.5 and 0.25, there are excess amounts of Cu component, which cannot be interpolated into Ag/Cu cores. They are deposited on the surfaces of Ag/Cu cores as Cu shells.

In Scheme 1a-1e are summarized possible growth mechanisms of Ag/Cu@Cu, Ag@Cu, Ag/Cu bicompartmental particles, hollow Cu particles and Cu@Ag particles obtained in our systematic studies using the same reagent under different experimental procedure and experimental conditions.[16-18] In processes (a) and (b), no Ag and Cu seeds are used, and Ag^+ and Cu^{2+} reagents are used. On the other hand, in processes (c)–(e), Ag or Cu seeds are prepared in the first step, and then Ag^+ or Cu^{2+} reagent is added in the second step. In process (a) used in this study, mixtures of Ag^+ and Cu^{2+} are injected to a hot EG solution, whereas in process (b) used in the previous study,[18] Ag^+ ions were injected after Cu^{2+} solution was kept at 175 °C. When Ag seeds with average diameters of 21±3 nm were prepared and then Ag^+ ions were added, Ag/Cu phase-separated particles with average diameters of 29±6 nm shown in process (c) are formed via melt of Ag seeds in high yield and no Ag@Cu core shell particles are formed.[17]

Here we discuss why Ag/Cu@Cu and Ag@Cu particles are produced through processes (a) and (b) although the same reagents and the same reaction temperature were used. In process (a), Cu^0 particles are absent in the initial stage, so that reaction (3) is insignificant. Under such conditions, Ag rich Cu alloy particles are initially produced through simultaneously reduction of Ag^+ and Cu^{2+} ions in EG. The reduction rate of Ag^+ is faster than that of Cu^{2+}, so that the reduction of Ag^+ is completed before the

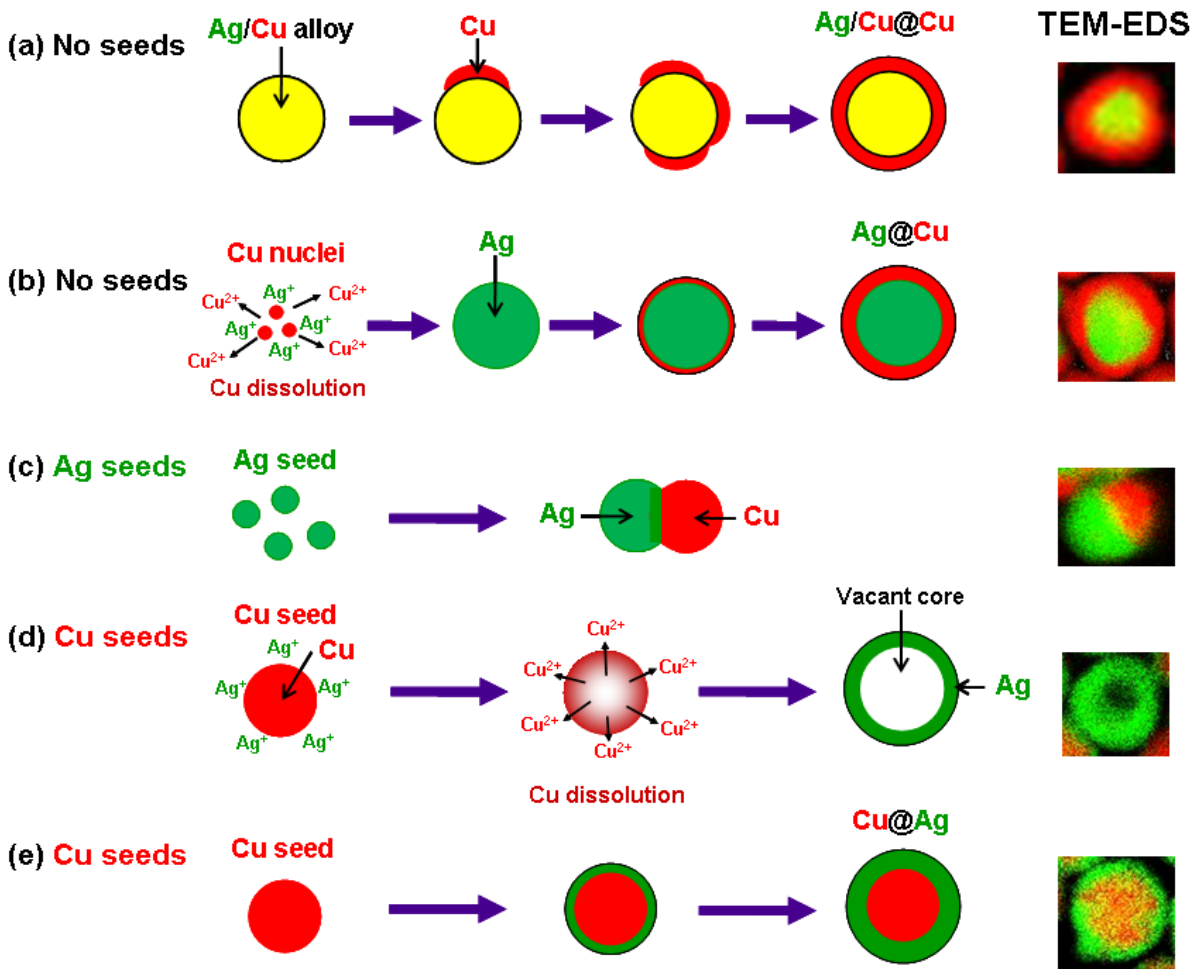

Scheme 1 Growth mechanism of (a) Ag/Cu@Cu, (b) Ag@Cu, (c) Ag/Cu bicompartmental, (d) hollow Ag (e) and Cu@Ag particles using polyol methods.

reduction of Cu^{2+} finishes. When the reduction of Ag^{+} is completed, the formation of Ag/Cu alloy particles stops. When excess amounts of Cu^{2+} are present, they are reduced on the surfaces of Ag/Cu cores and Cu shells are formed. In this case, since phase-separated structures are more stable than Ag@Cu core-shell structure having thin Cu shells, as observed in process (c), bi-, tri- and multi-compartmental particles are formed as intermediates in process (a). If there are sufficient amounts of Cu^{2+} ions, Ag/Cu alloy cores are fully covered by Cu shells.

When $AgNO_3$ was added to $Cu(OAc)_2{\cdot}H_2O$/EG/PVP solution preheated at 175 ^{o}C, Ag@Cu particles were produced in process (b).[18] By heating $Cu(OAc)_2{\cdot}H_2O$ solution to 175 ^{o}C, nucleation of Cu occurs so that very small Cu particles are probably produced. When $AgNO_3$ is added to such a Cu seeded solution, replacement reaction (3) takes place. Therefore, small Cu seeds are dissolved to Cu^{2+}, and Ag^{0} is dominantly produced through reaction (3) in the presence of Cu seeds. After all Ag^{+} ions are reduced to Ag^{0}, Cu^{2+} ions can be reduced to Cu^{0} on the surfaces of Ag core particles. Therefore Cu is not incorporated into the Ag core, and Ag@Cu particles are produced. The occurrence of replacement reaction (3) was confirmed by the addition of $AgNO_3$ to Cu core particles at low temperatures, where reaction (3) was faster than reaction (2a). Under such conditions, many hollow Ag particles are formed through process (d). When the reduction rate of Ag^{+} (2a) is sufficiently faster than that of replace reaction (3) at high temperature, Cu@Ag particles can be produced through process (e).[16] Our recently data show that product shapes of Ag-Cu bimetallic particles are very sensitive to experimental conditions. Therefore, the precise control of experimental conditions and procedures are necessary for the shape controlled syntheses of Ag-Cu particles.

Stability of Ag/Cu and Ag/Cu@Cu particles

UV-Vis spectra after preparation of Ag/Cu and Ag/Cu@Cu particles were measured to characterize optical properties and to examine oxidation rates of these particles (Fig. 7a-7d). Extinction spectra of pure Cu particles and Cu@Ag particles prepared using polyol methods are also shown in Fig. 7e and 7f for comparison. A SPR peak of Cu observed at ≈570 nm decreases rapidly with increasing time and almost disappears after 21 days owing to rapid oxidation (Fig. 7e). Extinction spectra of Cu@Ag obtained at an [Ag]/[Cu] molar ratio of 0.25 consist of strong Ag shell component in the 300–550 nm region with a peak at ≈430 nm and weaker Cu core component in the 550–800 nm region with a peak at ≈590 nm. The Ag shell peak at ≈430 nm decreases its intensity by a factor of 56% after 21 days, whereas the Cu core peak at

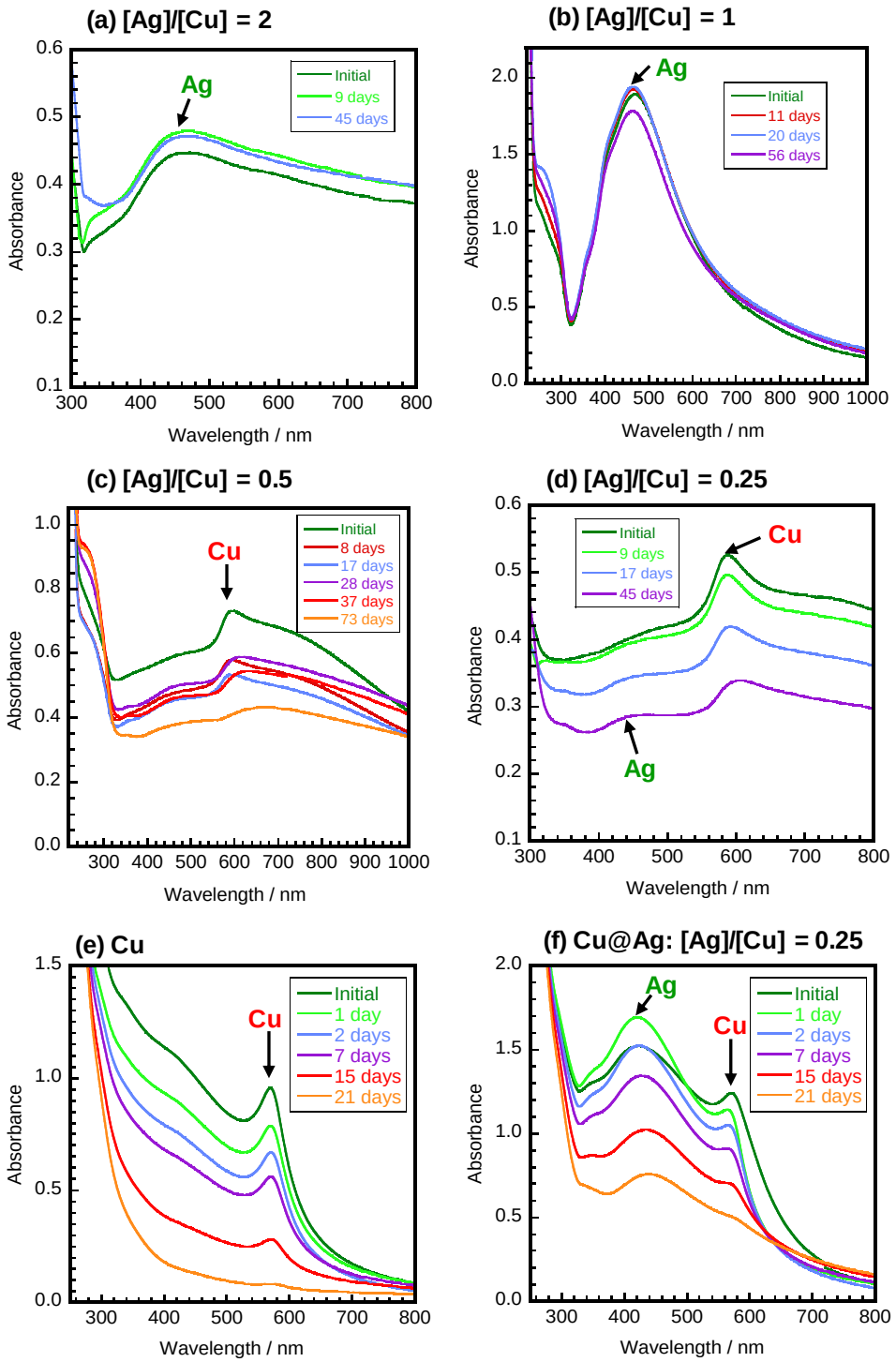

Fig. 7 (a)–(d) Time changes of UV-Vis spectra of Ag/Cu and Ag/Cu@Cu particles obtained at various Ag/Cu molar ratios after preparation. Similar time changes of (e) Cu and (f) Cu@Ag ([Ag]/[Cu] molar ratio = 0.25) particles are shown for comparison. Ag and Cu components in Ag/Cu, Ag/Cu@Cu and Cu@Ag are shown by arrows in (a)-(d) and (f).

≈590 nm decreases with increasing the time and almost disappears after 21 days because of rapid oxidation (Fig. 7f).

The time dependence of absorbance of Ag rich Ag/Cu alloy particles obtained at [Ag]/[Cu] molar ratios of 2 and 1 is shown in Fig. 7a and 7b, respectively The SPR peaks at ≈460 nm (Fig. 7a and 7b) due to Ag component decrease only slightly with increasing time. The slow decrease in the SPR peaks can be explained by the fact that alloy particles are mainly composed of Ag component (≈77 atomic %) having a high antioxidative property. The time dependence of absorbance of Ag/Cu@Cu particle obtained at [Ag]/[Cu] molar ratios of 0.5 and 0.25 is shown in Fig 7c and 7d, respectively. The absorbance of

Ag/Cu@Cu particles has a peak of Cu component at ≈590 nm and decreases its intensity by factors of 23 and 39% after 17 and 45 days, respectively, at an [Ag]/[Cu] molar ratio of 0.25. A similar slow reduction of Cu peak was observed at an [Ag]/[Cu] molar ratio of 0.5. These results show that, by covering Ag rich Ag/Cu cores with Cu shells, particle surfaces of Cu shells gained a higher antioxidative property than those of Cu and Cu@Ag particles.

Conclusion

For the preparation of new kind of core-shell particles, various mixtures of $AgNO_3$/$Cu(OAc)_2{\cdot}H_2O$/PVP were added to a hot solution of EG kept at 175 ^oC. Crystal structures of products were analyzed using TEM, TEM-EDS, SAED patterns and UV-Vis-NIR extinction spectra to obtain define information of product structures. We succeeded in the preparation of Ag rich Ag/Cu alloy and novel Ag/Cu@Cu particles. The crystal structures of products could be controlled by changing the [Ag]/[Cu] molar ratio or the reaction time. Ag rich Ag/Cu alloy particles could be obtained at high [Ag]/[Cu] molar ratios of 2 and 1 or at short reaction time at an [Ag]/[Cu] molar ratio of 0.25. On the other hand, Ag/Cu@Cu particles were obtained at low [Ag]/[Cu] molar ratios of 0.5 and 0.25 or at long reaction time. The thickness of Cu shells over Ag/Cu cores could be controlled by changing the [Ag]/[Cu] molar ratio or reaction time. We discussed the growth mechanisms of these particles and other related Ag@Cu, Cu@Ag, hollow Cu and Ag/Cu bicompartmental particles prepared in our group using the same reagents. We think that the procedure used in this study can be widely applied to the synthesis of A/B alloy core B shell particles, where the standard potential of metal A is higher than that of metal B and the reduction rate of A is much faster than that B.

We examined antioxidized properties of Ag/Cu@Cu particles and compared with those of Cu and Cu@Ag particles using the same apparatus. It was found that Ag/Cu@Cu particles possess higher antioxidized properties than those of Cu and Cu@Ag particles. Since drop by drop injection of $AgNO_3$ to Cu core solution is necessary for the production of Cu@Ag particles, mass production of Cu@Ag particles is difficult. On the other hand, Ag/Cu@Cu particles can be produced in a one-pot without using a titration technique, their mass production is easy. Thus, Ag/Cu@Cu particles are a new promising material including Cu.

Acknowledgements

We thank Mr. Takeshi Tanaka for his TEM–EDS measurements. This work was supported by the Joint Project of Chemical Synthesis Core Research Institutions, Grant-in-Aid for Scientific Research from the Japanese MEXT (Nos. 19033003, 19310064 and 22310060) and Kyushu University G-COE program "Novel Carbon Resource Sciences".

Notes and references

[a] *Institute for Materials Chemistry and Engineering, Kyushu University, Kasuga 816-8580, Japan. Fax: +81-092-583-7815; Tel: +81-092-583-7815; E-mail:tsuji@cm.kyushu-u.ac.jp*

[b] *Department of Applied Science for Electronics and Materials, Graduate School of Engineering Sciences, Kyushu University, Kasuga 816-8580, Japan*

[c] *Department of Energy Science and Engineering, Faculty of Engineering, Kyushu University, Kasuga 816-8580, Japan*

[d] *R & D Department, DIC Corporation, Sakura 285-8668, Japan*

† Electronic Supplementary Information (ESI) available: [A typical temperature profile of reagent solution after injection of $AgNO_3$/$Cu(OAc)_2{\cdot}H_2O$ into EG solution, TEM-EDS and its line analysis data of Ag@Cu particle and UV-Vis spectra of $AgNO_3$/$Cu(OAc)_2{\cdot}H_2O$/PVP reagent, and spherical Cu and Ag particles are shown.]. See DOI:10.1039/b000000x/

1 N. Toshima, *Pure Appl. Chem.*, 2000, **72**, 317.

2 J. H. Hodak, A. Henglein, M. Giersig and G. V. Hartland, *J. Phys. Chem. B*, 2000, **104**, 11708.

3 M. N. Nadagouda and R. S. Varma, *Cryst. Growth Des.*, 2007, **7**, 2582.

4 S. E. Habas, H. LEE, V. Radmilovic, G. A. Somorjai and P. Yang, *Nature Mater*., 2007, **6**, 692.

5 F.-R. Fan, D.-Y. Liu, Y.-F. Wu, S. Duan, Z.-X. Xie, Z.-Y. Jiang and Z.-Q. Tain, *J. Am. Chem. Soc*., 2008, **130**, 6949.

6 H. T. Zhang, J. Ding, G. M. Chow, M. Ran and J. B. Yi, *Chem. Mater*., 2009, **21**, 5222.

7 J.-W. Hu, J.-F. Li, B. Ren; D.-Y. Wu, S.-G. Sun and Z.-Q. Tian, *J. Phys. Chem. C*, 2007, **111**, 1105; S. Deng, K. C. Pingali and D. A. Rockstraw, *IEEE Sensors J*., 2008, **8**, 730; Y. Yang, J. Shi, G. Kawamura and M. Nogami, *Scr. Mater*., 2008, **58**, 862.

8 K. J. Majo, C. De and S. O. Obare, *Plasmonics*, 2009, **4**, 61.

9 M. Tsuji, N. Miyamae, S. Lim, K. Kimura, X. Zhang, S. Hikino and M. Nishio, *Cryst. Growth Des.*, 2006, **6**, 1801; M. Tsuji, R. Matsuo, P. Jiang, N. Miyamae, D. Ueyama, M. Nishio, S. Hikino, H. Kumagae, K. S. N. Kamarudin and X.-L. Tang, *Cryst. Growth Des.*, 2008, **7**, 2528; M. Tsuji, M. Nishio, P. Jiang, N. Miyamae, S. Lim, K. Matsumoto, D. Ueyama and X.-L. Tang, *Coll. & Surf. A*, 2008, **317**, 247; X.-L.Tang and M. Tsuji, *CrystEngComm.* submitted for publication.

10 M. Tsuji, Core *Shell Particles, in Shape and Structure Control of Metal Nano- and Fine-particles*, ed. by T. Yonezawa, CMC, Tokyo 2009, 166 (in Japanese).

11 H. Jiang, K.-S. Moon and C. P. Wong, *10th Int. Symp. Advpack. Mater: Process. Properties and Interfaces* 2005, 173.

12 M. Cazayous, C. Langlois, T. Oikawa, C. Ricolleau and A. Sacuto, *Phys. Rev. B* 2006, **73**, 113402; C. Langlois, D. Alloyeau, Y. L. Bouar, A. Loiseau, T. Oikawa, C. Mottet and C. Riolleau, *Faraday Discuss*., 2008, **138**, 375.

13 T. Nakamura, Y. Tsukahara, T. Yamauchi, T. Sakata, H. Mori and Y. Wada, *Chem. Lett.*, 2007, **36**, 154.

14 M. Grouchko, A. Kamyshny, K. Ben-Ami and A. S. Magdassi, *J. Nanopart. Res*., 2009, **11**, 713.

15 M. Singh, I. Sinha and R. K. Mandal, *Mater. Lett*., 2009, **63**, 2243.

16 M. Tsuji, S. Hikino, Y. Sano and M. Horigome, *Chem. Lett.*, 2009, **38**, 518.

17 M. Tsuji, S. Hikino, R. Tanabe and Y. Sano, *Chem. Lett*., 2009, **38**, 860

18 M. Tsuji, S. Hikino, R. Tanabe and D. Yamaguchi, *Chem. Lett.*, 2010, **39**, 334.

19 Y. Xiong, I. Washio, J. Chen, H. Cai, Z.-Y. Li and Y.Xia, *Langmuir*, 2006, **22**, 8563.

20 M. Tsuji, S. Kumagae, M. Matsunaga, X.-L. Tang, R. Tanabe and M. Ogino, to be published.

21 M. Tsuji, M. Hashimoto, Y. Nishizawa, M. Kubokawa and T. Tsuji, *Chem. Eur. J*., 2005, **11**, 440.

22 A. Henglein and G. Giersig, *J. Phys. Chem.*, 1994, **98**, 6931.

Figure captions.

Fig. 1 TEM and TEM-EDS data of Ag-Cu bimetallic particles prepared from $AgNO_3$/$Cu(OAc)_2 \cdot H_2O$/PVP mixtures in EG at [Ag]:[Cu] molar ratios of (a) 2:1, (b) 1:1, (c) 0.5:1 and (d) 0.25:1.

Fig. 2 Distributions of Ag and Cu along cross section lines shown in Fig. 1(a)-1(d).

Fig. 3 Ag-Cu bimetallic particles prepared from $AgNO_3$/$Cu(OAc)_2 \cdot H_2O$/PVP mixtures in EG at an [Ag]/[Cu] molar ratio of 0.25 after heating for (a) 5 min, (b) 17.5 min and (c) 27 min.

Fig. 4 Distributions of Ag and Cu along cross section lines shown in Fig. 3(a)-3(c).

Fig. 5 SEAD patterns of Ag-Cu bimetallic products prepared from $AgNO_3$/$Cu(OAc)_2 \cdot H_2O$/PVP mixtures in EG at an [Ag]/[Cu] molar ratio of 0.25 after heating for (a) 5 min, (b) 17.5 min and (c) 27 min.

Fig. 6 (a)–(d) Time changes of UV-Vis spectra of Ag/Cu and Ag/Cu@Cu particles obtained at various [Ag]/[Cu] molar ratios after preparation. Similar time changes of (e) Cu and (f) Cu@Ag ([Ag]/[Cu] molar ratio = 0.25) particles are shown for comparison.

Fig. 7 (a)–(d) Time changes of UV-Vis spectra of Ag/Cu and Ag/Cu@Cu particles obtained at various Ag/Cu molar ratios after preparation. Similar time changes of (e) Cu and (f) Cu@Ag ([Ag]/[Cu] molar ratio = 0.25) particles are shown for comparison. Ag and Cu components in Ag/Cu, Ag/Cu@Cu and Cu@Ag are shown by arrows in (a)-(d) and (f).

Scheme 1 Growth mechanism of (a) Ag/Cu@Cu, (b) Ag@Cu, (c) Ag/Cu bicompartmental, (d) hollow Ag (e) and Cu@Ag particles using polyol methods.

A table of contents entry (Synopsis for Graphical Abstract)
Figure for Graphical Abstract

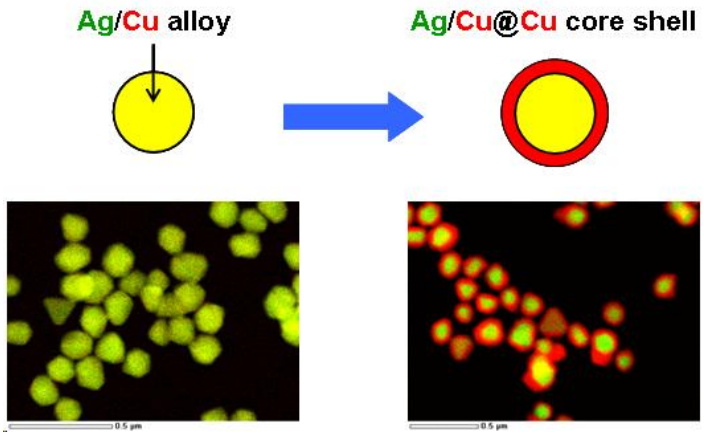

Text: one sentence, of maximum 20 words, highlighting the novelty of the work.

Ag/Cu alloy core Cu shell nanoparticles having high antioxidized properties were synthesized using a polyol method.

Supplementary Information

Syntheses of Ag/Cu alloy and Ag/Cu alloy core Cu shell nanoparticles using a polyol method

Masaharu Tsuji,*[a,b,c] Sachie Hikino,[a] Ryuichi Tanabe,[b] Mika Matsunaga[c] and Yoshiyuki Sano[d]

[a]*Institute for Materials Chemistry and Engineering, Kyushu University, Kasuga 816-8580, Japan,*

[b]*Department of Applied Science for Electronics and Materials, Graduate School of Engineering Sciences, Kyushu University, Kasuga 816-8580, Japan,*

[c]*Department of Energy Science and Engineering, Faculty of Engineering, Kyushu University, Kasuga 816-8580, Japan,*

[d]*R & D Department, DIC Corporation, Sakura 285-8668, Japan*

*To whom correspondence should be addressed: E-mail: tsuji@cm.kyushu-u.ac.jp

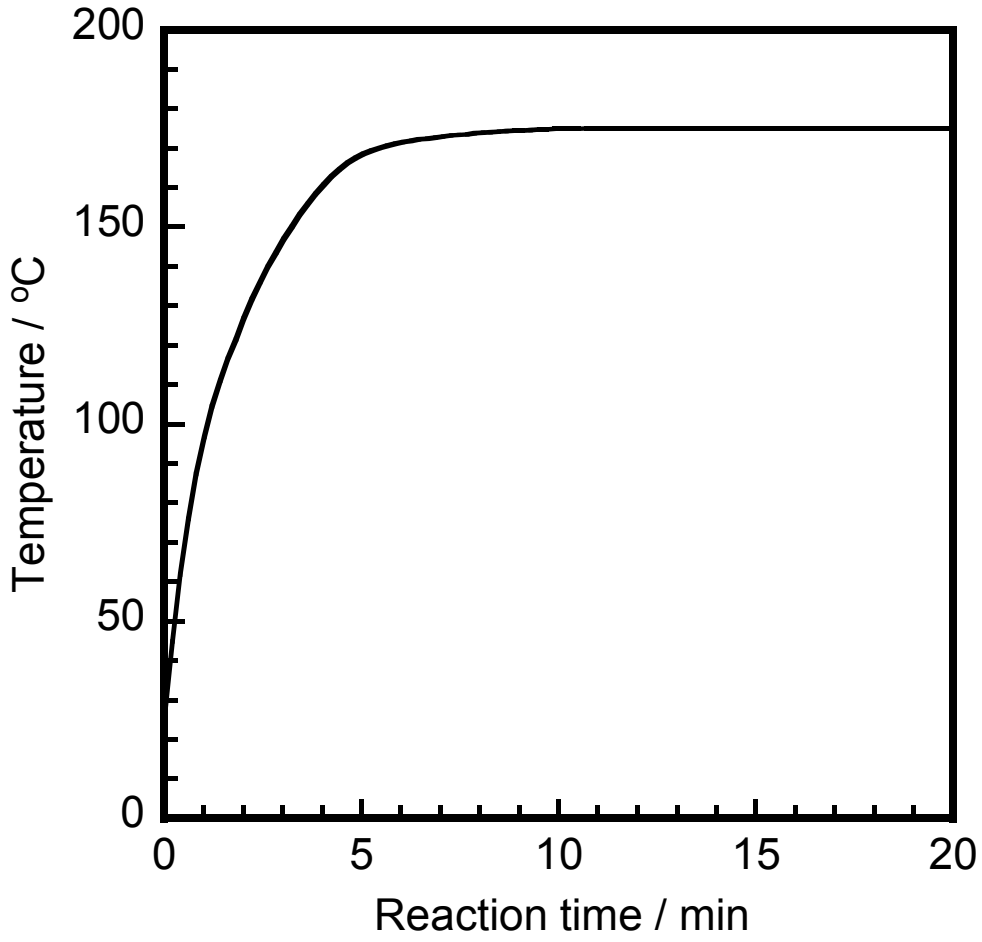

Fig. S1 Temperature profile of reagent solution after injection of $AgNO_3$/$Cu(OAc)_2 \cdot H_2O$/PVP mixtures.

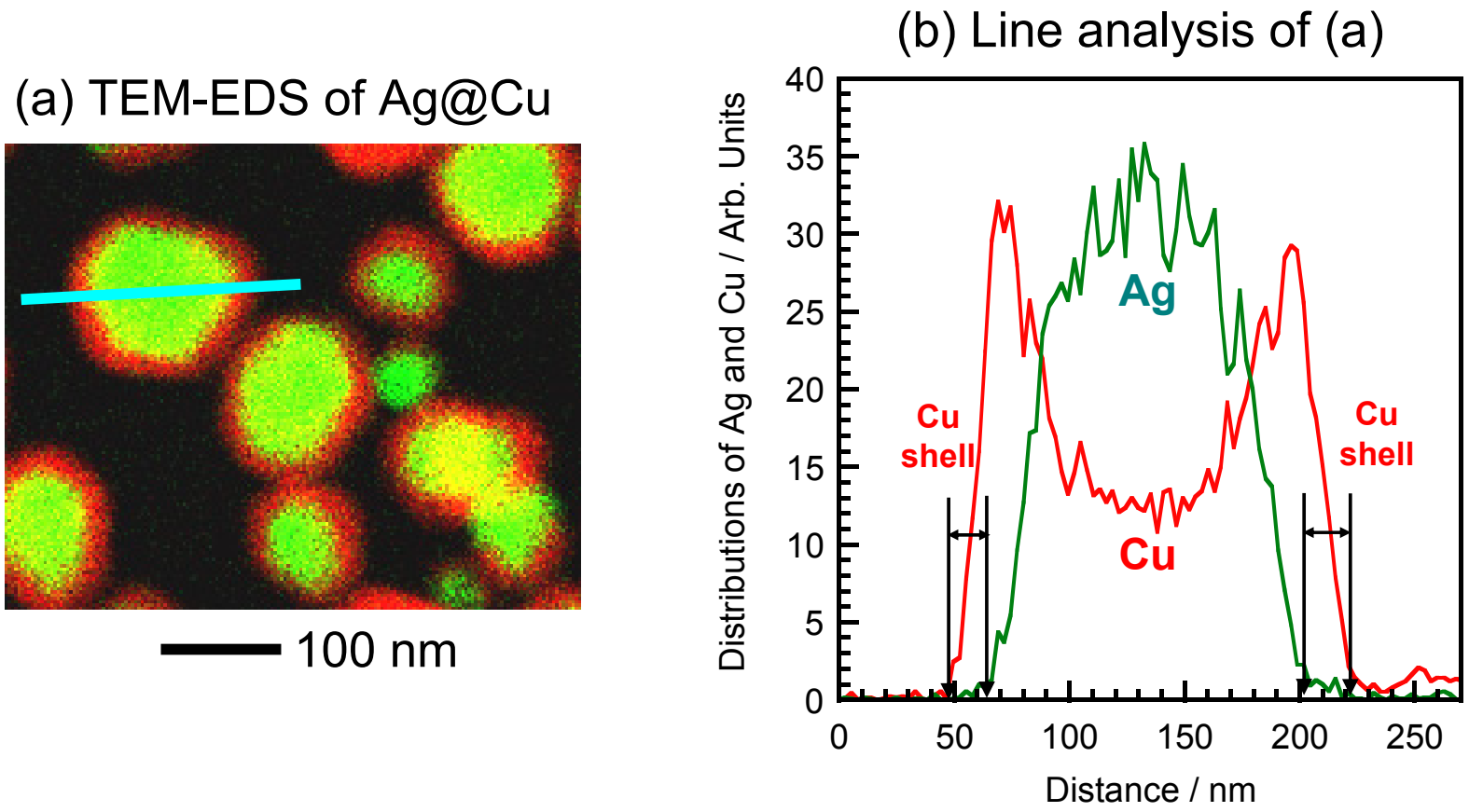

Fig. S2 (a) TEM-EDS of Ag@Cu particles and (b) its line analysis along cross section line shown in (a).

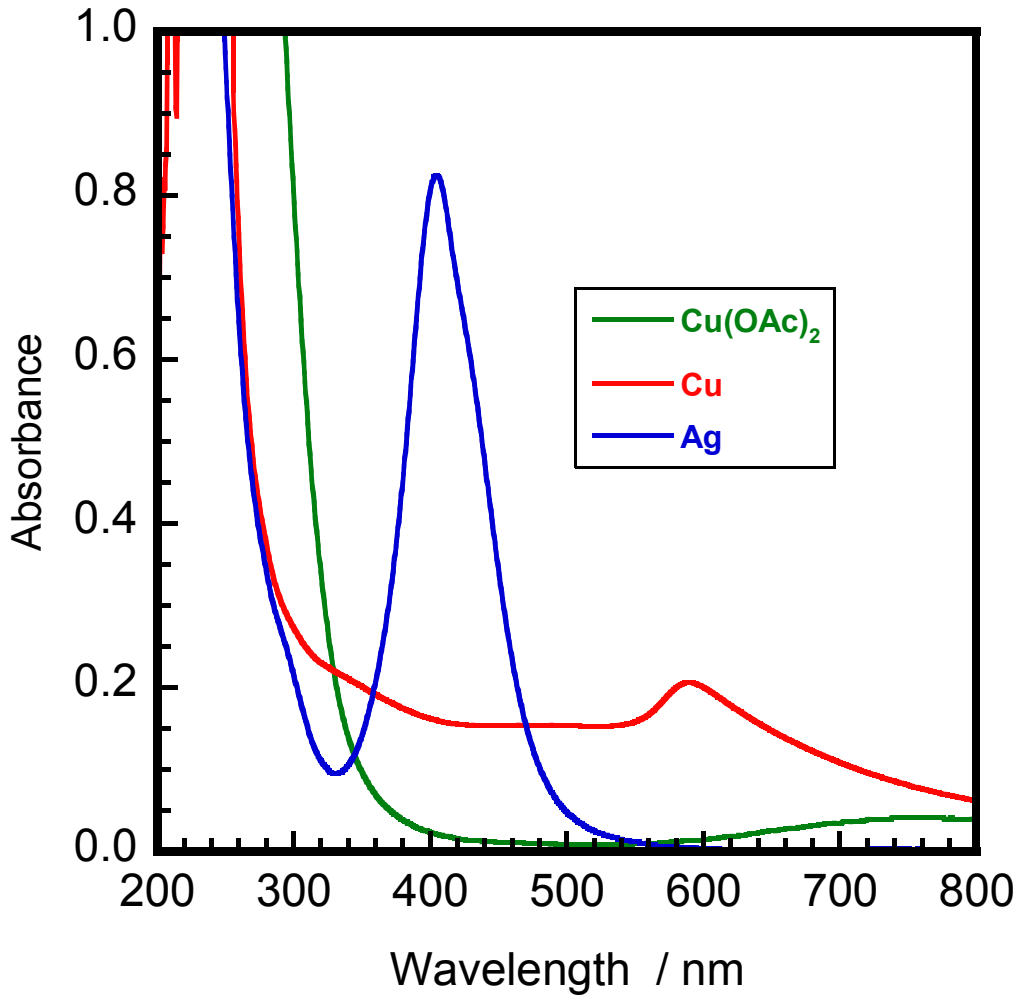

Fig. S3 UV-Vis extinction spectra of $Cu(OAc)_2$, Cu particles, and Ag particles.